Phase-locked laser system for use in atomic coherence experiments

Alberto M. Marino[a] and C. R. Stroud, Jr.
The Institute of Optics, University of Rochester, Rochester, New York 14627, USA

(Received 18 July 2007; accepted 19 November 2007; published online 11 January 2008)

We describe a phase-coherent laser system designed for use in experiments involving coherently prepared atomic media. We implement a simple technique based on a sample-and-hold circuit together with a reset of the integrating electronics that makes it possible to scan continuously the relative frequency between the lasers of over tens of gigahertz while keeping them phase locked. The system consists of three external-cavity diode lasers operating around 795 nm. A low-power laser serves as a frequency reference for two high-power lasers which are phased locked with an optical phase-locked loop. We measured the residual phase noise of the system to be less than 0.04 rad^2. In order to show the application of the system towards atomic coherence experiments, we used it to implement electromagnetically induced transparency in a rubidium vapor cell and obtained a reduction in the absorption coefficient of 92%. © *2008 American Institute of Physics.*
[DOI: 10.1063/1.2823330]

I. INTRODUCTION

The pioneering work on optical phase locking was done in the 1960s;[1,2] however, it was not until the 1980s that most of the development took place with the implementation of homodyne and heterodyne optical phase locking.[3] It is now possible to obtain phase-locked lasers with a residual phase noise of only 1 μrad in a 10 Hz bandwidth.[4] The ability to produce phase-coherent lasers through techniques such as optical phase-locked loops (OPLLs) has lead to important advances in coherent optical communications, precision spectroscopy, frequency stabilization of lasers, and heterodyne and homodyne detection.[5]

More recently, one of the applications for phase-coherent lasers has been in the field of quantum optics for the generation of coherently prepared media. The importance of atomic coherence resides in the fact that it can be used to modify the optical response of a medium. As a result, it is possible to use this effect for the enhancement of nonlinear processes,[6] lasing without inversion,[7,8] slow light,[9,10] and the generation of continuous variable entanglement that is needed for applications such as teleportation[11,12] and quantum communications.[13,14]

One of the effects that has a direct impact on the amount of atomic coherence that can be generated in a system is the relative fluctuation of the phase between the lasers used to generate the coherence. In order to minimize this effect, it is necessary to use phase-coherent lasers in any experiment based on atomic coherence. When possible, what is done is to use a single laser and obtain all the necessary frequencies for the experiment by using either an acousto-optic modulator (AOM) or an electro-optic modulator (EOM). However, this is not possible when the frequency separation between the fields is large or when large tuning ranges are needed. In these cases, the use of an OPLL is required to stabilize the relative frequency and phase between two lasers and obtain the required phase coherence.

When working with atomic systems it is sometimes necessary to scan continuously the relative frequency between two lasers over a Doppler broadened spectrum of several gigahertz while still maintaining the phase coherence. For this purpose phase-locked laser systems that can scan in discrete steps[15] or continuously[16] have been recently developed. In this article we describe a simple method for implementing a phase-coherent laser system that makes it possible to scan continuously the relative frequency between lasers of over tens of gigahertz. To demonstrate the use of such a system for the generation of atomic coherence, we present, as an example, electromagnetically induced transparency (EIT) experiments[17,18] in a Λ system in the D1 line of ^{87}Rb in a vapor cell.

II. LASER SYSTEM

In order to obtain phase-coherent lasers and overcome the limitations that result from using either an AOM or an EOM, we implemented the laser system shown in Fig. 1. The system consists of three external-cavity diode lasers (ECDLs) operating around 795 nm. Referring to Fig. 1, the reference laser (RL) is a low-power laser that serves as a frequency reference for locking two high-power lasers. The frequency of one of the high-power lasers, the master laser (ML), is locked directly to the RL using an optical phase-locked loop (OPLL), as will be described later. The second high-power laser, the slave laser (SL), is phase locked to the ML using another OPLL. This configuration allows us to have accurate control over the frequency difference between the two high-power phase-coherent lasers. By using the setup shown in Fig. 1, we are able to obtain two high-power phase-coherent lasers that can be independently tuned over a wide

[a]Current address: National Institute of Standards and Technology, Gaithersburg, Maryland 20899 USA. Electronic mail: alberto.marino@nist.gov.

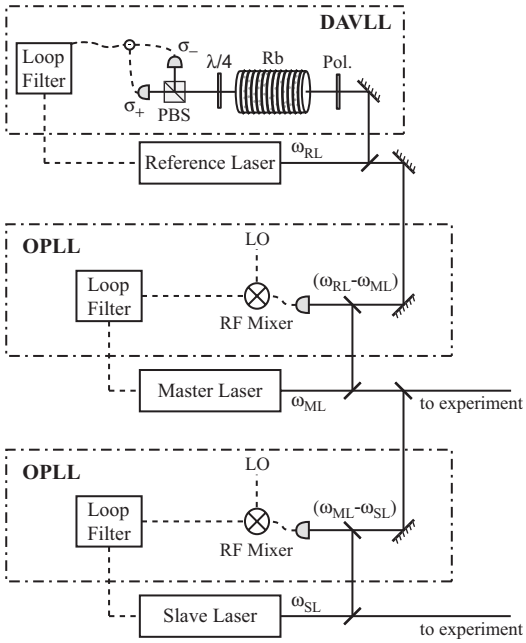

FIG. 1. Schematic of laser system. The system consists of three external-cavity diode lasers. The reference laser serves as an optical frequency reference used to stabilize two high-power lasers. The frequency of the master laser is stabilized with respect to the reference laser through the use of an optical phase-locked loop. The slave laser is phased locked to the master laser by using another optical phase-locked loop.

range. In general, the tuning range of the lasers is only limited by the electronics used for the OPLL and can be as large as tens of gigahertz.

For the implemented laser system, the low-power RL is a New Focus Vortex laser, model 6017. This laser uses a Littman-Metcalf configuration[19] which gives a short-term linewidth of 300 kHz, provides up to 18 mW of output power, and has a mode-hop free tuning range of 60 GHz. The ML is a Toptica TA100 laser system which consists of an ECDL and a tapered amplifier. The ECDL in this system is based on the Littrow configuration[20,21] such that it has a short-term linewidth of 1 MHz. The total output power from the ML is 500 mW and its mode-hop free tuning range is around 10 GHz. Finally, the SL is a Toptica DLX110 laser system in which the diode laser and amplifier are in a single structure. This laser is also based on the Littrow configuration, can provide up to 400 mW of output power, and has a mode-hop free tuning range of around 15 GHz.

The absolute frequency stability of the laser system shown in Fig. 1 is determined by the RL, which serves as the optical frequency reference for the two high-power lasers. In order to obtain a good absolute frequency stability, the RL was locked to an absorption line of Rb by using the dichroic atomic vapor laser locking (DAVLL) technique.[22–24] This technique consists of propagating a linearly polarized portion of the output of the laser to be stabilized through a Rb cell that has an applied magnetic field along the direction of the laser beam propagation. After the cell a polarization analyzer is used to measure the transmission of the right- and left-hand circular polarization components of the fields. Finally, the difference of the measured photocurrents is obtained. The resulting difference signal depends linearly on the laser frequency in the vicinity of the atomic resonance. This signal can be used as the error signal to stabilize the laser. The main reason this technique was selected for the stabilization of the RL is its simplicity and the fact that it offers a large capture and locking range.

For the actual implementation of the DAVLL technique a beam sampler is used to pick off a small portion of the RL with a power of 130 μW. The required magnetic field is obtained by using permanent ring magnets mounted on both sides of a 10 cm long Rb cell. The magnetic field provided by the permanent magnets is of the order of 50 G. For our experiments, the RL is usually locked to the zero crossing that corresponds to the $F=2\rightarrow F'$ transition of ^{85}Rb. The constant slope regime for this transition has a width of around 550 MHz. As a result of such a large width, a very robust locking to the atomic absorption line is obtained. Due to the large locking range provided by the DAVLL technique, once the RL is locked it remains locked for several hours. If better absolute frequency stability is required, other methods such as saturation spectroscopy can be used to stabilize the frequency of the RL.

Fluctuations in the number density of Rb atoms in the cell can affect the locking obtained with the DAVLL technique. Such fluctuations result from temperature drifts. In order to minimize this effect, the Rb cell used for the DAVLL scheme was temperature stabilized by using a home-built feedback circuit based on a temperature controller, model WTC3243, from Wavelength Electronics. This circuit provides a temperature stability of at least ±0.5 °C

III. OPTICAL PHASE-LOCKED LOOP

In order to stabilize the frequency and phase of the lasers, it is necessary to have both a slow and a fast mechanism to compensate for any frequency fluctuations. The slow feedback channel is provided by the piezoelectric transducer (PZT) control of the diffraction grating or mirror of the ECDL. This channel typically has a modulation bandwidth of 2–3 kHz and is capable of compensating for large frequency fluctuations. This channel can be used to compensate for slow temperature drifts or mechanical vibrations which can generate substantial frequency fluctuations.

The fast feedback channel is provided by the injection current of the diode laser. When the injection current of the diode laser is changed, both the diode's temperature and the carrier density in the semiconductor are changed. As a result, a corresponding change in the index of refraction of the diode laser occurs that is responsible for a change in its operating frequency. This channel can provide a modulation bandwidth that goes from a few megahertz to a few gigahertz, depending on the electronics used to modulate the injection current. In general, in order to avoid large modulations in the output power, the feedback channel provided by the injection current is used only to compensate for the higher frequency fluctuations which are typically small in amplitude.

The frequency and phase of the ML and SL are stabilized by implementing an OPLL (Refs. 5 and 25) for each of the lasers. A typical OPLL, shown in Fig. 2, is composed of

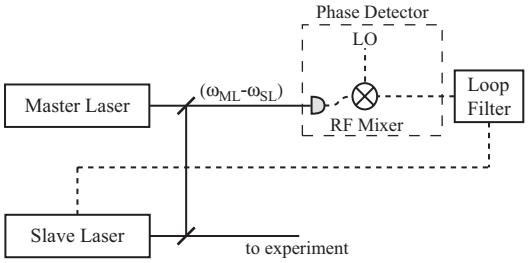

FIG. 2. Schematic of an optical phase-locked loop. An optical phase-locked loop consists of a master laser, a slave laser, a phase detector, and a loop filter.

four main parts: a ML, a SL, a phase detector, and a loop filter. The ML serves as the frequency and phase reference for the SL. In order to obtain information on the frequency and phase difference between the lasers, the ML and the SL are mixed with a beam splitter and the beat signal detected with a photodiode which serves as the phase detector. The resulting beat-note signal contains the relevant information about the frequency and phase difference between the lasers, thus providing the error signal needed by the feedback loop to compensate for any deviations in frequency and phase between the lasers. If it is necessary for the lasers to operate at different frequencies, then a LO must be used to mix down the beat-note signal from the photodiode. In this case, the LO will determine the frequency difference between the two lasers and can be used to tune the frequency of the SL relative to the ML.

In general, for an OPLL, the residual phase-error variance depends on the linewidths of the lasers and the noise bandwidth of the feedback system. For the case of a second-order feedback loop, the phase-error variance is given by[5]

$$\Delta\phi^2 = \frac{2(\Delta\nu_M + \Delta\nu_S)}{B_F}, \tag{1}$$

where $\Delta\nu_M$ and $\Delta\nu_S$ are the linewidths of the ML and SL, respectively, and B_F is the noise bandwidth of the feedback loop. The noise bandwidth of the feedback system needs to be large enough to reduce the residual phase noise of the system below a predetermined value that depends on the specific application. Typically $\Delta\phi^2 < 0.1$ rad^2 is required, such that the noise bandwidth of feedback system has to be at least an order of magnitude larger than the sum of the linewidths of the lasers. One of the main complications of implementing an OPLL is the large magnitude of the laser phase noise or linewidth; as a result, a very fast feedback system is required. For the ECDLs used for the ML and SL the linewidths are of the order of 1 MHz. As a result, the feedback loop needs to have a noise bandwidth of 20 MHz or more.

In order to implement the OPLL required for the laser system described in Fig. 1, a number of different electronic components were used. The phase detector is composed of several elements. First, a high speed photodetector from EOT, model ET-4000, with a bandwidth of 10 GHz is used to detect the beat-note signal between the lasers. After the detector, a bias-T, Taylor Microwave model BT-A06, is used to separate the dc portion of the beat-note signal from the high-frequency component which contains the information required by the feedback electronics. The dc portion of the signal is used to monitor the power of the lasers. The high-frequency portion of the signal then goes through a high speed amplifier, Miteq model AFS2, which has a gain of 15 dB and a bandwidth from 0.5 to 10 GHz. In order to phase lock the lasers with a frequency separation between them, a mixer, Remec model MM96P6-40 (rf/LO bandwidth from 0.5 to 18 GHz and IF bandwidth from dc to 300 MHz), and a LO are used. After the mixer the error signal is fed into the feedback electronics.

The required frequency separation between the two high-power lasers is obtained by using an Agilent microwave signal generator, model E8247C, as the LO in the OPLL. Since microwave signal generators allow for an accurate control of their frequency, a very precise control over the frequency separation between the two lasers can be obtained. The Agilent microwave signal generator allows us to perform a ramp scan of its output frequency, such that the frequency of the LO can be continuously scanned from 250 kHz to 20 GHz. This makes it possible to scan continuously the relative frequency between the lasers while the lasers remain phase locked. The Agilent microwave signal generator has a frequency resolution of 0.001 Hz.

The schematic for the feedback electronics that we designed and implemented for the OPLL is shown in Fig. 3. In order to obtain the required bandwidth for the feedback system, we need both the slow and fast channels for frequency control of the ECDL. The upper half of the design corresponds to the electronics used for the slow portion of the feedback. The control signal that results from this part of the electronics is applied to the input in the ECDL that controls the PZT. The lower portion of the design corresponds to the feedback electronics for compensating the fast phase fluctuations of the laser. The output of this section of the circuit is applied to the input that modulates the injection current of the diode laser. The use of both slow and fast feedback channels requires careful design at the crossover frequency. At this point both channels have the same gain so that their action on the system is comparable. If the combined response of the two channels is not properly designed the system can become unstable.

Due to the large amplitude of the slow frequency fluctuations of the ECDL, the actual implementation of the OPLL is more complicated than previously described. One of the problems of using the phase detector composed of a photodetector and mixer is that the resulting error signal is not linear, it is a sinusoidal signal. This limits the range over which the error signal can be used to a range of less than π. The large amplitude of the slow frequency fluctuations resulting from mechanical vibration and temperature drifts are enough to drive the phase detector to its nonlinear regime. As a result, the use of both a digital phase detector for the slow frequency fluctuations as well as an analog mixer for the fast frequency fluctuations is required.[26] The digital phase detector offers a linear response over a range of 4π, making it capable of compensating for larger phase fluctuations between the lasers. In addition, the digital phase detector can also act as a frequency comparator, such that it makes it

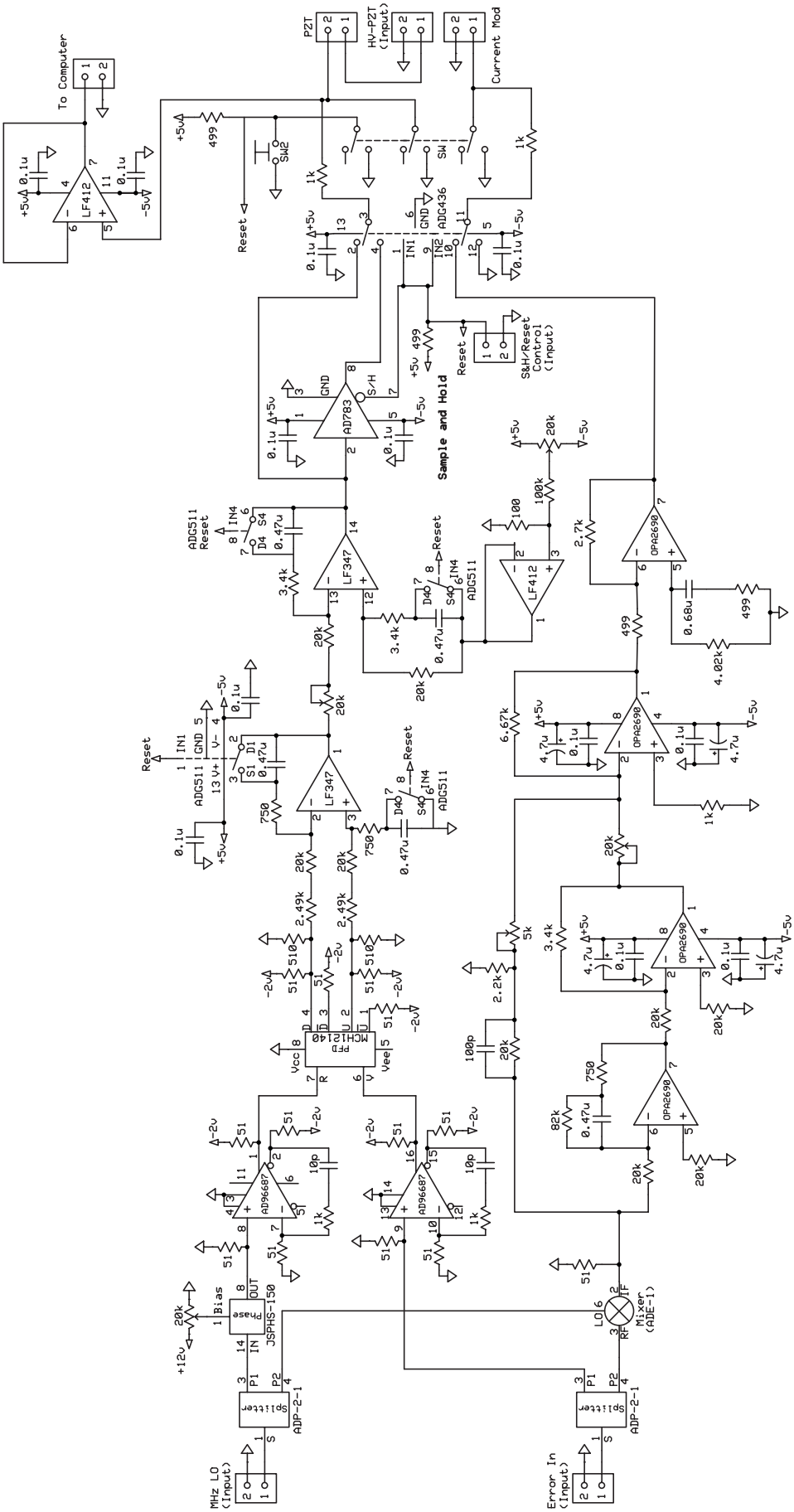

FIG. 3. Schematic of feedback electronics designed for the OPLL used to stabilize the frequency and phase of the master and slave lasers.

possible for the feedback system to compensate for the large frequency drifts of the ECDL. However, one of the problems of using a digital phase detector is the noise introduced due to the digitization of the signal. This makes it necessary to combine both digital and analog devices in the same design.

The digital phase detector, model MCH12140, requires the use of an additional LO at around 100 MHz as a reference signal. In order to implement this, the high speed photodetector together with the mixer and the Agilent microwave signal generator are used to downshift the beat-note or error signal to 125 MHz. Then a splitter is used to separate the error signal into two parts, one going to the digital phase detector and the other to an analog mixer, Mini-Circuits model ADE-1. An additional signal generator, HP model 8647A, is used to provide the necessary LO for the digital phase detector. This second LO is fixed at a frequency of 125 MHz and is also split into two portions, one for the digital phase detector and one for the analog mixer. In order to use the digital phase detector, the 125 MHz LO and the corresponding error signal are digitized with the use of high speed comparators, model AD96687. Once this is done, both digital signals are fed into the digital phase detector which gives as an output a square wave signal whose duty cycle is proportional to either the frequency or phase difference between the lasers. In order to extract the duty cycle, the digital signal is integrated, thus providing the error signal. The feedback electronics then uses this signal in order to apply the necessary compensation to the PZT input of the ECDL. For the high speed portion of the feedback circuit, the 125 MHz LO and the corresponding error signal are combined in the analog mixer to bring the error signal down to dc. This in turn gives the necessary error signal for the feedback electronics used to compensate for the fast fluctuations through the current modulation input of the ECDL.

The combination of digital and phase detectors requires special attention to the relative phase between the LO and the error signal. The MCH12140 will tend to lock the system such that the LO and the error signals are in phase, while the analog phase detector will lock them in quadrature. As a result, the LOs must be 90° out of phase. This is achieved with a phase shifter, model JSPHS-150, before the digital phase detector.

The OPLL and electronics described above are used in order to stabilize the frequency difference between the RL and the ML and also to phase lock the SL to the ML in the laser system described in Fig. 1. In order to stabilize the frequency between the RL and the ML, only the slow portion of the feedback system is required since the digital phase detector provides enough bandwidth to compensate for slow temperature drifts and mechanical vibrations that may affect the frequency of the ML. The phase locking of the SL to the ML requires the implementation of both the slow and fast portions of the feedback system as previously described.

One of the reasons the Agilent microwave signal generator was chosen as the LO for the OPLL is its ability to perform a ramp scan of its output frequency. This allows us to continuously tune the frequency separation between the ML and RL while keeping the system phase locked. One of the problems with scanning over large frequency ranges with any microwave signal generator is that it needs to reset its internal electronics at certain frequencies in order to obtain the required scan range. During these resets, the microwave signal generator gives no output signal or the output is not stable, which results in the OPLL losing its lock due to the lack of a reference signal or LO. In order to overcome this problem and obtain a large tuning range while maintaining the phase lock, we implemented some modifications to the typical OPLL described above. First, a sample-and-hold circuit, model AD783, was included at the output stage of the electronics. As a result, whenever there is a reset of the LO, the circuit is set to its hold mode in order to avoid the lasers from drifting from their current operating frequency. In order to avoid a drift of the feedback electronics, specifically of the integrating stages, the output of the signal generator that indicates that it was resetting was used to reset all the integration stages in the electronics by using an analog switch, model ADG511. During the resets of the LO the system will momentarily lose lock. However, due to the sample-and-hold circuit and the resetting of the integrating stages, the drift of the feedback system will be minimal such that when the LO continues its scan the system will immediately reacquire lock. As a result of these two additions, it is, in principle, possible to scan over a range that is only limited by the microwave signal generator and the phase detector used.

In addition, in order to compensate for the scanning ramp voltage that needs to be applied to the PZT for tuning the laser and avoid saturation of the feedback electronics, the scanning ramp from the signal generator is captured with a computer with a data acquisition card. The measured signal is then conditioned and applied to the laser controller such that the required scanning ramp voltage is applied directly to the laser and does not need to be compensated by the feedback system. This way, the feedback system only needs to compensate for the frequency and phase fluctuations between the lasers. With these methods, we have been able to use the OPLL to scan the frequency of the SL with respect to the ML over a frequency range of 1.4 GHz while still keeping the lasers phase locked. We limited the maximum scan rate of the system to 300 MHz/s when performing our experiments in order to avoid transient effects when generating atomic coherence using EIT, as will be described in Sec. V.

IV. RESULTS

In order to characterize the OPLL, we measured the spectrum of the beat-note signal between the ML and SL (see Fig. 4). Fig. 4(a) shows the beat-note signal when the lasers are only frequency locked, curve (i), and when the lasers are phased locked, curve (ii). For these measurements the spectrum analyzer was set to resolution and video bandwidths of 10 kHz and the frequency separation between the ML and SL was 6.02 GHz. The beat-note signal for the case in which the lasers are only frequency locked is obtained by using only the slow portion of the feedback system. From this measurement we find that the beat-note has a full width at half maximum (FWHM) of around 1.5 MHz. When the fast portion of the feedback system is also used, the beat note narrows down dramatically, an indication that the lasers are

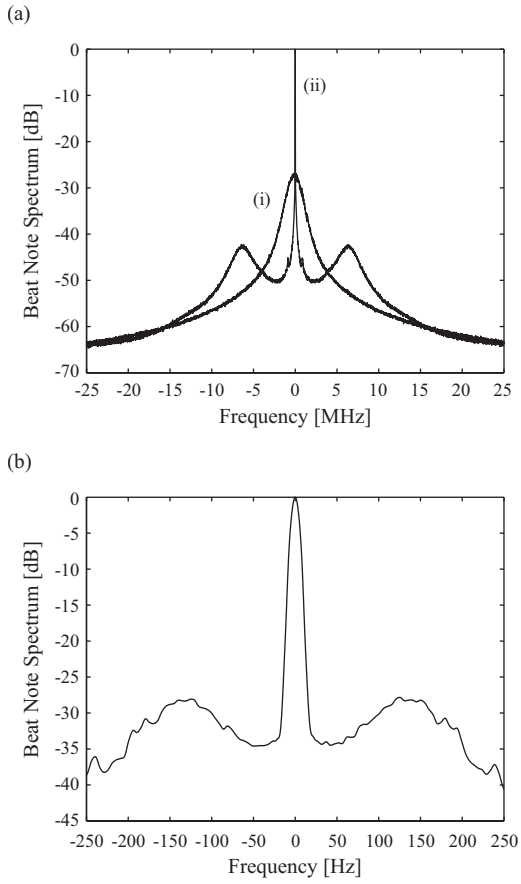

FIG. 4. Measured beat-note signal between master and slave lasers. (a) Curve (i) shows the beat-note signal when only the relative frequency between the master and slave lasers is stabilized while curve (ii) shows the beat-note signal when the lasers are phase locked (resolution/video bandwidth=10 kHz). The effect of the OPLL is to narrow down the beat-note signal. (b) Expanded view around the narrow beat-note signal that is obtained with the OPLL (resolution/video bandwith=10 Hz).

phase locked. In this case, most of the power is concentrated in the narrow beat-note signal, which is 25 dB higher than in the case of only frequency-stabilized lasers. The two broad peaks on either side of the narrow beat note are due to a reduced phase margin as the gain of the feedback loop tends to unity. However, these peaks are over 40 dB below the peak of the beat-note signal. In order to get a better estimate of the performance of the OPLL, we zoom in around the narrow beat-note signal, Fig. 4(b), to measure its width. For this measurement the spectrum analyzer was set to its highest resolution and video bandwidth, that is, 10 Hz. From the result obtained, the width of the phase-locked beat note (FWHM) is measured to be 10 Hz; however, this measurement is limited by the resolution bandwidth of the spectrum analyzer, so that the beat-note signal is narrower than this.

The effective noise bandwidth of the OPLL can be estimated to be around 7 MHz from the broad peaks in the beat-note signal between the phase-locked lasers, Fig. 4(a). The crossover frequency between the slow and fast channels of the feedback system is around 130 Hz. At this point, the difference in the response between the two channels leads to the broad peaks around the narrow beat note shown in Fig. 4(b).

The residual phase noise of an OPLL is a direct indication of the performance of the feedback system. This quantity can be experimentally obtained from the fraction of power, η, contained in the narrow beat-note signal. For the case in which the mean-square phase error is small, $\Delta\phi^2 \ll 1$, η is given by[27,28]

$$\eta = \frac{P(0)}{\int_{-\infty}^{\infty} P(f)df} = \exp(-\Delta\phi^2), \tag{2}$$

where $P(0)$ is the power in the narrow beat-note signal and the integral in the denominator represents the total power in the signal. From the results presented in Fig. 4, the residual phase noise can be calculated such than $\Delta\phi^2 < 0.04$ rad^2. As mentioned above, this measurement is limited by the resolution bandwidth of the spectrum analyzer.

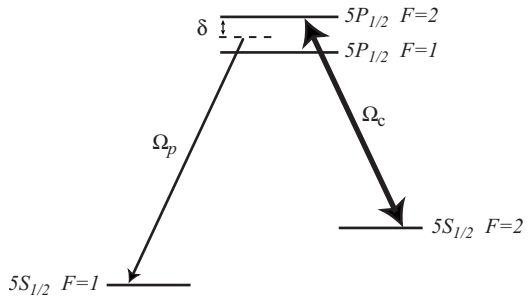

FIG. 5. Atomic configuration used for EIT measurements in ^{87}Rb.

V. ELECTROMAGNETICALLY INDUCED TRANSPARENCY IN ^{87}Rb

In order to test the performance of the system for the generation of atomic coherence and show its tuning capabilities, we implemented EIT in a Λ system in the D1 line of ^{87}Rb. The amount of reduction in the absorption coefficient gives an indication of how well the laser system can prepare an atomic system in a coherent superposition of the ground states of the atom. In order to perform the EIT measurements in ^{87}Rb, the ML was tuned to the $F=2 \rightarrow F'=2$ transition and served as the control field in the EIT configuration. The probe field was obtained from the SL and was tuned to the corresponding transition of the Λ system, as shown in Fig. 5. The frequency of the probe field can be tuned with respect to the control field by using the OPLL, as previously described. In order to measure the reduction in absorption due to EIT, the probe field was scanned over a range of 1.4 GHz while keeping the lasers phase locked. This scanning range is enough to scan over the whole Doppler broadened transition and thus allowed us to measure the absolute change in transmission resulting from EIT. A typical EIT curve obtained from these measurements is shown in Fig. 6(a). For the measurements shown in this figure, curve (i), the control field had a power of 16.5 mW while the power of the probe field was 843 μW. The temperature of the cell was set to 91 °C, which corresponds to a number density of around 2.6×10^{12} cm^{-3}. The central feature at the Raman resonance condition, $\delta=0$, corresponds to the effect of atomic coherence in the system. As we can see from Fig. 6(a), the measurement results show how the transmission drastically

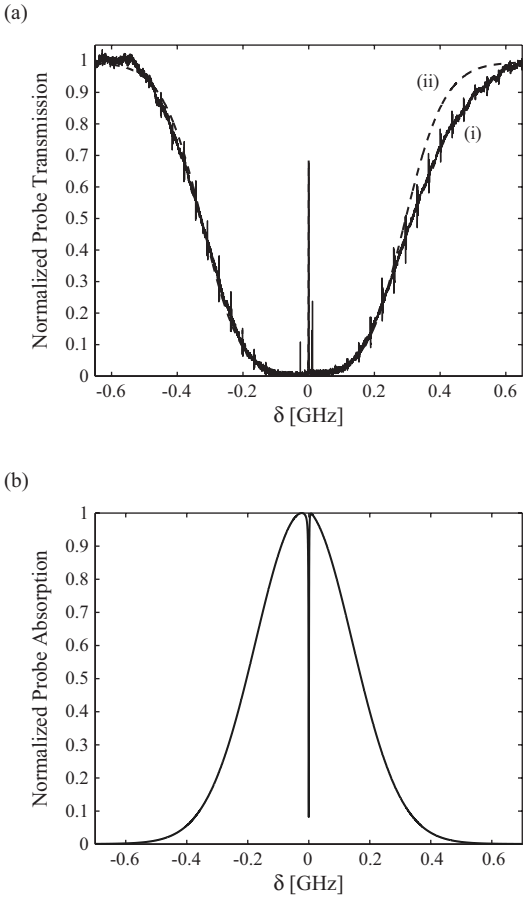

FIG. 6. EIT signal in ^{87}Rb. (a) shows the measured, curve (i), and calculated, curve (ii), transmission spectrum for the probe beam. The use of phase-locked lasers made it possible to obtain a contrast of 70%. The periodic structure in the transmission spectrum is due to discrete signal used in OPLL to compensate for the frequency scanning ramp. (b) shows the calculated absorption spectrum corresponding to the measured transmission spectrum. A reduction in the absorption coefficient of 92% was obtained.

changes from the probe being absorbed to about 70% transmission. The periodic structure that appears in the figure is due to the digital compensation that is applied to the control box of the SL in order to achieve a large tuning range while maintaining the lasers phase locked. Since the compensation signal is discrete, each time there is a change in the level of the compensation signal the system momentarily looses lock, as a result, the scan has a periodic structure. This effect can be eliminated if a continuous, instead of the discrete signal, is used to compensate for the scanning ramp.

For the case of copropagating beams, ignoring residual Doppler broadening ($\omega_c \simeq \omega_p$), the Doppler averaged susceptibility for the probe beam due to EIT in a Λ system can be shown to be of the form[29]

$$\chi^{\text{dopp}} = \frac{i2\sqrt{2\pi \ln 2}\mathcal{N}|d_{32}|^2}{\epsilon_0 \hbar \Delta\omega_D} e^{-z^2} \operatorname{erfc}(-iz), \tag{3}$$

where $\mathcal{N}$ is the number density, d_{32} is the dipole matrix element of the probe transition, $\Delta\omega_D$ is the Doppler broadened linewidth (FWHM), erfc is the complementary error function, and

$$z = \frac{2\sqrt{2 \ln 2}}{\Delta\omega_D}\left(\Delta - \delta + i\gamma_{32} + \frac{|\Omega_c|^2/4}{\delta - i\gamma_{21}}\right). \tag{4}$$

Here, γ_{32} is the dipole dephasing rate of the optical transition for the probe beam, γ_{21} is the decoherence rate between the two ground states, Δ is the single-photon detuning, and δ is the Raman detuning. In order to obtain transparency the susceptibility has to be as small as possible at Raman resonance; that is, we need to have $|z| \gg 1$. This implies, for the case $\Delta = \delta = 0$, that the following condition needs to be satisfied:

$$\frac{|\Omega_c|^2}{4\gamma_{21}\Delta\omega_D} \gg 1. \tag{5}$$

That is, the Rabi frequency of the control field needs to be large enough to overcome any decoherence between the ground states.

The experimental parameters given above were used in the Doppler averaged susceptibility, Eq. (3), to calculate the expected probe transmission, shown in curve (ii) of Fig. 6(a). As we can see, the agreement between the calculated and measured probe transmission spectra is very good. The asymmetry in the measured transmission curve is due to the other excited state hyperfine level in the D1 line of ^{87}Rb. From this calculation, we can estimate the ground state decoherence rate γ_{21} to be of around 100 kHz. We can use this result to model the absorption spectrum that corresponds to the measured transmission spectrum. By using the calculated Doppler averaged susceptibility to obtain the absorption coefficient, we find that a reduction in the absorption level of 92% was obtained, as shown in Fig. 6(b). This result shows that the implemented system was able to generate a superposition between the atomic ground states, or atomic coherence.

VI. DISCUSSION

We have presented a phase-coherent laser system designed for use in experiments with coherently prepared media. We have shown how it is possible to scan continuously the relative frequency between the lasers of over tens of gigahertz while keeping the lasers phase locked with the use of a sample-and-hold circuit together with a reset of the integrating stages of the feedback electronics. This simple technique makes it possible, for example, to scan over a Doppler broadened atomic spectrum for applications such as spectroscopy or characterization of effects based on atomic coherence.

We were able to obtain a system with a residual phase noise of less than 0.04 rad^2. In order to demonstrate the use of the implemented system for atomic coherence experiments and show its scanning capabilities, we performed EIT experiments. For these experiments, the relative frequency between the lasers was continuously scanned over 1.4 GHz. In addition, we were able to obtain a reduction in absorption of 92%.

[1] P. Rabinowitz, J. LaTourrette, and G. Gould, Proc. IEEE **51**, 857 (1963).
[2] L. H. Enloe and J. L. Rodda, Proc. IEEE **53**, 165 (1965).
[3] J. L. Hall, M. Long-Sheng, and G. Kramer, IEEE J. Quantum Electron. **23**, 427 (1987).
[4] J. Ye and J. L. Hall, Opt. Lett. **24**, 1838 (1999).

[5] M. Ohtsu, *Highly Coherent Semiconductor Lasers* (Artech House, Boston, 1992).
[6] H. Schmidt and A. Imamoglu, Opt. Lett. **21**, 1936 (1996).
[7] S. E. Harris, Phys. Rev. Lett. **62**, 1033 (1989).
[8] M. O. Scully, S. Y. Zhu, and A. Gavrielides, Phys. Rev. Lett. **62**, 2813 (1989).
[9] L. V. H. Hau, S. E. Harris, Z. Dutton, and C. H. Behroozi, Nature (London) **397**, 594 (1999).
[10] M. M. Kash, V. A. Sautenkov, A. S. Zibrov, L. Hollberg, G. R. Welch, M. D. Lukin, Y. Rostovtsev, E. S. Fry, and M. O. Scully, Phys. Rev. Lett. **82**, 5229 (1999).
[11] S. L. Braunstein and H. J. Kimble, Phys. Rev. Lett. **80**, 869 (1998).
[12] A. Furusawa, J. L. Sørensen, S. L. Braunstein, C. A. Fuchs, H. J. Kimble, and E. S. Polzik, Science **282**, 706 (1998).
[13] C. Silberhorn, N. Korolkova, and G. Leuchs, Phys. Rev. Lett. **88**, 167902 (2002).
[14] A. M. Marino and C. R. Stroud, Jr., Phys. Rev. A **74**, 022315 (2006).
[15] H. Müller, S. Chiow, Q. Long, and S. Chu, Opt. Lett. **31**, 202 (2006).
[16] P. Cheinet, F. Pereira Dos Santos, T. Petelski, J. Le Gouët, J. Kim, K. T. Therkildsen, A. Clairon, and A. Landragin, Appl. Phys. B: Lasers Opt. **84**, 643 (2006).
[17] S. E. Harris, J. E. Field, and A. Imamoglu, Phys. Rev. Lett. **64**, 1107 (1990).
[18] J. P. Marangos, J. Mod. Opt. **45**, 471 (1998).
[19] K. C. Harvey and C. J. Myatt, Opt. Lett. **16**, 910 (1991).
[20] L. Ricci, M. Weidemuller, T. Esslinger, A. Hemmerich, C. Zimmermann, V. Vuletic, W. Konig, and T. W. Hansch, Opt. Commun. **117**, 541 (1995).
[21] A. S. Arnold, J. S. Wilson, and M. G. Boshier, Rev. Sci. Instrum. **69**, 1236 (1998).
[22] K. L. Corwin, Z. T. Lu, C. F. Hand, R. J. Epstein, and C. E. Wieman, Appl. Opt. **37**, 3295 (1998).
[23] M. A. Clifford, G. P. T. Lancaster, R. S. Conroy, and K. Dholakia, J. Mod. Opt. **47**, 1933 (2000).
[24] V. V. Yashchuk, D. Budker, and J. R. Davis, Rev. Sci. Instrum. **71**, 341 (2000).
[25] F. M. Gardner, *Phaselock Techniques* (Wiley, New York, 1966).
[26] L. Cacciapuoti, M. de Angelis, M. Fattori, G. Lamporesi, T. Petelski, M. Prevedelli, J. Stuhler, and G. M. Tino, Rev. Sci. Instrum. **76**, 053111 (2005).
[27] M. Zhu and J. L. Hall, J. Opt. Soc. Am. B **10**, 802 (1993).
[28] M. Prevedelli, T. Freegarde, and T. W. Hansch, Appl. Phys. B: Lasers Opt. **B60**, S241 (1995).
[29] J. Gea-Banacloche, Y. Q. Li, S. Z. Jin, and M. Xiao, Phys. Rev. A **51**, 576 (1995).